Ionics (2013) 19:771–776
DOI 10.1007/s11581-012-0798-5

ORIGINAL PAPER

Improvement of a novel anode material TeO_2 by chlorine doping

Ya Wang · Hai-Long Fei

Received: 12 June 2012 / Revised: 26 July 2012 / Accepted: 19 August 2012 / Published online: 12 September 2012

Abstract A simple and versatile method for the preparation of chlorine-doped TeO_2 was developed via thermal decomposition of $Te_6O_{11}Cl_2$ in situ. $Te_6O_{11}Cl_2$ was prepared with $TeCl_4$ and ethanol as reagents, while TeO_2 was fabricated with water as a solvent. The morphology, surface, and electrochemical performances of the obtained materials were systematically studied. It was found that chlorine-doped TeO_2 demonstrated the highest cycling efficiency and stability than $Te_6O_{11}Cl_2$ and TeO_2. The presence of Te–Cl bond is expected to contribute to the reversible capacity and Li inserting process.

Keywords TeO_2 · $Te_6O_{11}Cl_2$ · Anode·lithium-ion battery · Chlorine doping

Introduction

The Te (IV)-containing compounds have attracted much interest, owing to various excellent properties related to macroscopic polarization and polarisability (dielectric, piezoelectric, optic, and electroacoustic), which are of great interest to fundamental science and technology [1]. Among these compounds, amorphous TeO_2 and alpha-TeO_2 (paratellurite) have attracted much attention for their various important applications, such as in gamma-ray sensor [2] and temperature-stable SAW device [3]. Also, TeO_2-based glasses are potential materials for upconversion and thermometric [4], non-linear optical [5], and waveguide devices application [6].

But Te-containing compounds were seldom used as energy storage materials. Recently, the cathodic capacity of $LiMn_2O_4$ has been promoted via narrow range of nano-Te doping [7]. Krins et al. investigated the relationship between the structural characteristics of the xLi_2O $(1-x)(0.3\ V_2O_5–0.7\ TeO_2)$ system and its electrical behavior [8]. But single-phased tellurium oxide (TeO_2) has not been reported to be tested as lithium-ion battery electrode material, as far as we know. It is well-known that TeO_2 crystal contains cavities and tunnels [1]. Furthermore, Te exhibits multiple covalent bonds. So it may be used as lithium-inserting electrode material. Until now, great attention has been drawn to prepare amorphous TeO_2 film/nanoparticles [9–13] and tellurium oxides by various methods [14].

Herein, we develop a simple and versatile method for the preparation of TeO_2 and study its electrochemical performance as anode material for lithium-ion battery. By careful adjustment of the synthesis parameters, $Te_6O_{11}Cl_2$ and TeO_2 microcrystals were controllably fabricated with ethanol and water as solvent, respectively. The corresponding chlorine-doped TeO_2 was prepared via thermal decomposition of the precursor of $Te_6O_{11}Cl_2$ in situ. When used as anode material for lithium-ion batteries, chlorine-doped TeO_2 shows the best electrochemical properties than TeO_2 and $Te_6O_{11}Cl_2$. The possible reason is that the Te–Cl bond in TeO_2Cl_x promotes formation of lithium–tellurium alloy. This facile method to fabricate chlorine-doped TeO_2 would be of great significance to design other chlorine-doped lithium-ion battery electrode material with advanced functions.

Experimental

Preparation and characterizations of materials

All chemicals are commercially available and used without further purification. In a typical procedure, 3 g of $TeCl_4$ was dissolved in 30 ml absolute ethanol and stirred at room temperature for 30 min, and then the mixed solution was

Y. Wang · H.-L. Fei (✉)
Institute of Advanced Energy Materials, Fuzhou University, Fuzhou 350002, China
e-mail: fimer99@yahoo.com.cn

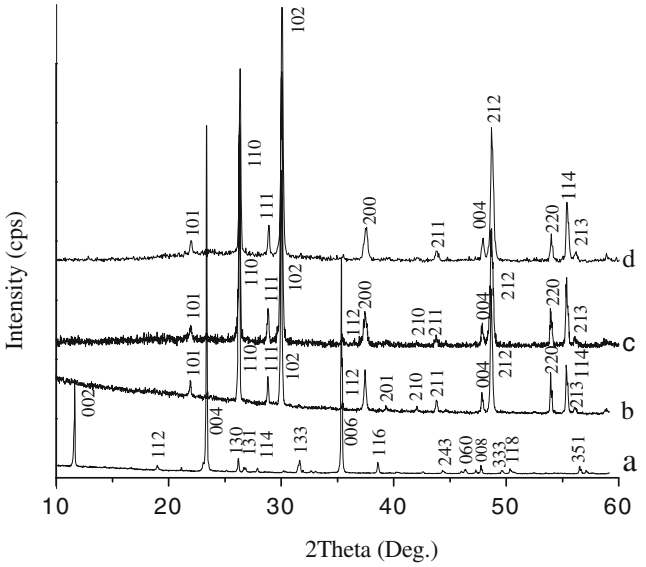

Fig. 1 XRD patterns of the as-synthesized products prepared with ethanol (sample Tol-1) (**a**), the calcining product of sample Tol-1 (sample Tol-1c) (**b**), the as-synthesized product prepared with water (sample Toh-2) (**c**) and the calcined product of Sample Toh-2 (Sample Toh-2c) (**d**)

transferred into a 50-ml Teflon-lined stainless autoclave and kept at 200 °C for 24 h. After the reaction was finished, it was cooled to room temperature. The precursors were filtered, washed with absolute ethanol, and dried at 60 °C for 12 h. The dried precursor (denoted as Sample Tol-1) was calcined at 400 °C for 3 h with a heating rate of 5 °C/min to get Sample Tol-1c. When 30 ml deionized water was added to take the place of ethanol, sample Toh-2 was obtained under the identical condition, which was calcined at 400 °C for 3 h to get sample Toh-2c. $TeCl_4$ is toxic and handle with utmost care.

The morphology of products was observed by Hitachi S-4800 field emission scanning electron microscope. X-ray diffraction (XRD) patterns were recorded on a diffractometer (Co Kα, PANalytical, X'Pert, data were convert into Cu Kα). X-ray photoelectron spectroscopy (XPS) measurements were performed with an Escalab 250 spectrometer.

The electrochemical properties

$Te_6O_{11}Cl_2$ (Sample Tol-1), TeO_2 (Sample Toh-2 and Toh-2c) and chloride-doped TeO_2 (Sample Tol-1c) were used as anode materials for lithium-ion battery. The negative electrode was prepared via pasting slurries of active materials, acetylene black, and polyvinylidene fluoride with a weight ratio of 6:3:1 on a Cu foil circular flake. The flake was dried at 120 °C for 12 h under vacuum condition. The metallic lithium foil was used as the positive electrode. The electrolyte was 1 M $LiPF_6$ in the mixed solvent of ethylene carbonate, dimethyl carbonate, and diethylene carbonate with a volume ratio of 1:1:1. All cells were assembled in an argon-filled glove box. Charge–discharge cycles were performed with a Land CT 2001A cycle life tester (Wuhan, China) at a current density of 20 $mA\,g^{-1}$ in the voltage range between 0.05 and 3.0 V versus Li/Li^+. Chloride-doped TeO_2 (sample Tol-1c) was tested in the voltage from 0.05 to 3.0 V and successively discharged at the current density of 60, 120, 180, 240, 300, and 360 $mA\,g^{-1}$. Cyclic voltammetry (CV) experiments were performed using a CHI660 and Zahner IM6 electrochemical work station at a scan rate of 1 $mV\,s^{-1}$.

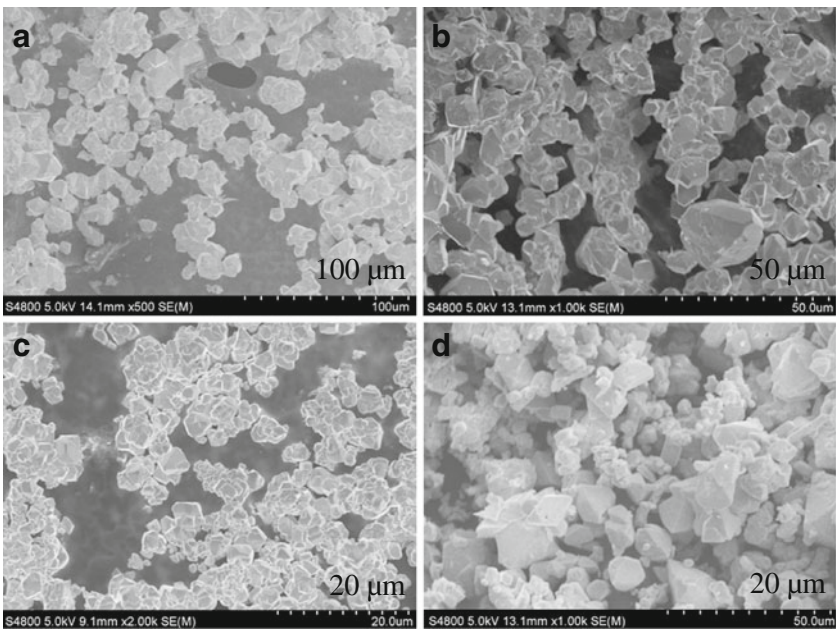

Fig. 2 SEM images of $Te_6O_{11}Cl_2$ (sample Tol-1) (**a**), TeO_2Cl_x (sample Tol-1c) (**b**), the as-synthesized (sample Toh-2) and calcined TeO_2 (sample Toh-2c) prepared with water (**c**, **d**), respectively

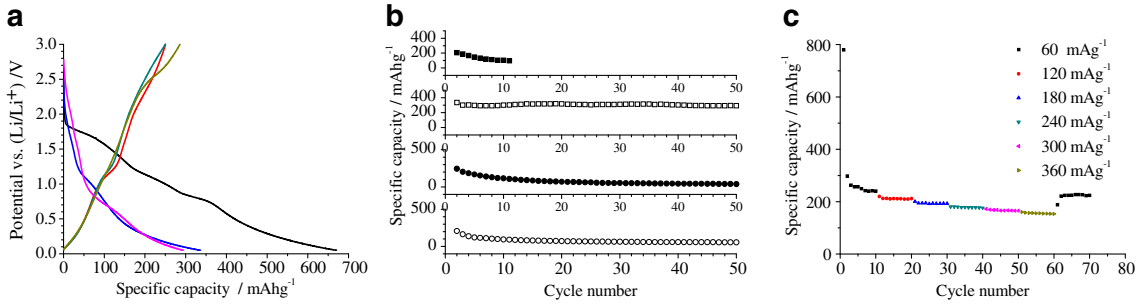

Fig. 3 The discharge–charge curves of TeO_2Cl_x (sample Tol-1c) (**a**), the cycle performance of $Te_6O_{11}Cl_2$ (*filled square*, sample Tol-1), TeO_2Cl_x (*white square*, sample Tol-1c), the as-synthesized TeO_2 prepared with water (*filled circle*, sample Toh-2) and the calcined TeO_2 prepared with water (*white circle*, sample Toh-2c) (**b**) and the evolution of the reversible capacity for TeO_2Cl_x (sample Tol-1c) at different current densities (**c**)

Results and discussion

Crystalline structure and morphologies of samples

The structural information is provided by XRD, as shown in Fig. 1. It can be found that solvent has a dramatic effect on the crystalline structure of products. The precursor prepared with ethanol (sample Tol-1) is crystalline $Te_6O_{11}Cl_2$ (JCPDS 85-2305) in Fig. 1a, while that obtained with water (sample Toh-1) is ascribed to Paratellurite TeO_2 (JCPDS 11-0693), as shown in Fig. 1c. The possible reason might be ascribed to the formation of different tellurium precursors in different solvents. It was reported that $TeCl_4$ could react with ethanol to form $TeCl_{4-x}(OC_2H_5)_x$ [15], which was further transformed to $Te_6O_{11}Cl_2$. It was also reported that $Te_6O_{11}Cl_2$ could be prepared with TeO_2, H_2O, and HCl as reagents [16]. But no H_2O or HCl was involved in our experimental procedure. After calcinations, both $Te_6O_{11}Cl_2$ and TeO_2 were converted to alpha-TeO_2 (sample Toh-1c and Toh-2c) (JCPDS 84-1777), as shown in Fig. 1b, d, respectively.

Scan electron microscopy (SEM) was performed to investigate the obtained four samples. The as-synthesized $Te_6O_{11}Cl_2$ and TeO_2 have similar morphologies as shown in Fig. 2a, b, which are all mono-dispersed irregular microcrystals about dozens of micrometers in size. After calcinations, the obtained TeO_2 has a similar morphology to the as-synthesized $Te_6O_{11}Cl_2$ and TeO_2 in Fig. 2c, d, respectively.

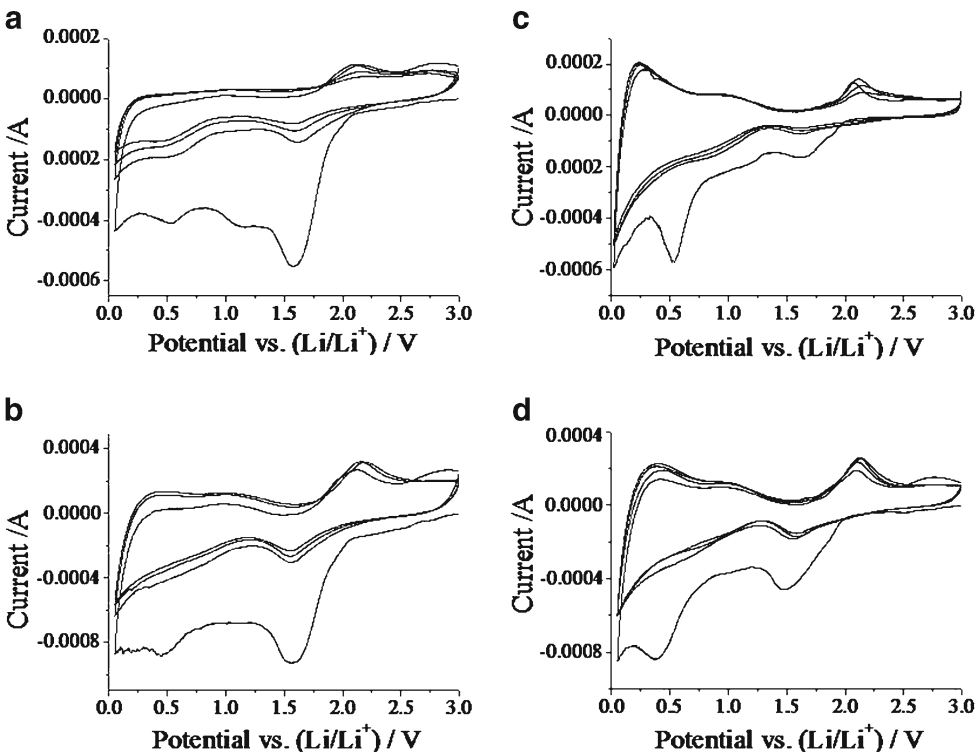

Fig. 4 CV curves of $Te_6O_{11}Cl_2$ (sample Tol-1) (**a**), the as-synthesized TeO_2 prepared with water (sample Toh-2) (**b**), TeO_2Cl_x (sample Tol-1c) (**c**) TeO_2 prepared with water after calcinations (sample Toh-2c) (**d**), respectively

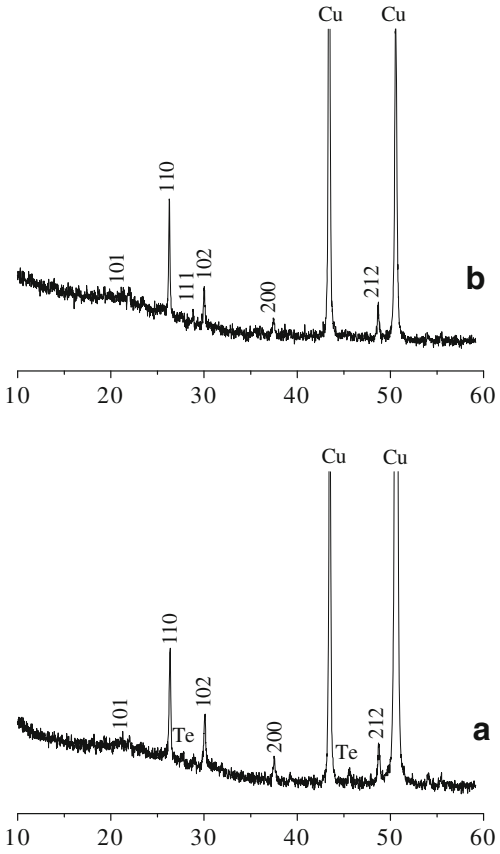

Fig. 5 XRD patterns of TeO_2Cl_x (sample Tol-1c) discharged at 0.3 (**a**) and 1.5 V (**b**), respectively

Electrochemical performances

TeO_2 (sample Toh-2 and Toh-2c) and $Te_6O_{11}Cl_2$ (sample Tol-1) and chloride-doped TeO_2 (TeO_2Cl_x, sample Tol-1c) were tested as anode materials for lithium-ion battery. The corresponding cyclic performance is shown in Fig. 3b. It can be clearly seen that $Te_6O_{11}Cl_2$ and the as-synthesized and calcined TeO_2 prepared with water as solvent exhibit relative low discharge capacity and bad cycling stability in Fig. 3b (marked with filled square, filled circle, and white circle, respectively). While chlorine-doped TeO_2 (TeO_2Cl_x, Sample Tol-1c) exhibits high discharge capacity and good cycle stability in Fig. 3b (marked with white square). The corresponding discharge profiles at a discharge current of 20 $mA\,g^{-1}$are shown in Fig. 3a. The initial, 1st, and 50th discharge capacity is 670.3, 336.1, and 294.2 $mAh\,g^{-1}$, respectively. The corresponding discharge rate capability of chlorine-doped TeO_2 (TeO_2Cl_x, sample Tol-1c) is tested at a current density of 60, 120, 180, 240, 300, and 360 mA g^{-1} (Fig. 3c), which exhibits stable discharge capacity at various discharge rates.

Cyclic voltammetry (CV) was further performed to investigate electrochemical properties of $Te_6O_{11}Cl_2$ and TeO_2 prepared with different precursors, as shown in Fig. 4. The first CV cycle of $Te_6O_{11}Cl_2$ (Sample Tol-1) exhibits one strong cathodic peak at 1.65 V and a weak one at 0.52 V (Fig. 4a), which is same to that of the as-synthesized (sample Toh-2) and calcined TeO_2 (sample Toh-2c) prepared with water in Fig. 4c and d. But the first CV curve of TeO_2 prepared with $Te_6O_{11}Cl_2$ (sample Tol-1c) exhibits one strong cathodic peak at 0.52 and a weak one at 1.65 V (Fig. 4a). However, all the four samples exhibit same CV curves for the second, third, and fourth cycle with one weak cathodic peak at 1.65 V.

X-ray diffraction was further performed to investigate the crystalline structure of TeO_2 prepared with $Te_6O_{11}Cl_2$ (sample Tol-1c) discharged from 3 to 1.5 and 0.3 V. The results show that the product discharged at 1.5 V is crystalline TeO_2 (Fig. 5a), while that at 0.3 V is mixed-phase of TeO_2 and Te (Fig. 5b). Therefore, the cathodic peak at 0.52 V can be ascribed to lithium–tellurium alloy (Li_xTe), while that at 1.65 V might be ascribed to Li_xTeO_2. TeO_2 prepared from $Te_6O_{11}Cl_2$ (Sample Tol-1c)exhibits better electrochemical properties due to inhibit Li_xTeO_2 formation and promote to formation of lithium–tellurium alloy (Li_xTe), the latter will favor good electrochemical performance.

XPS was performed to determine the state of the element on the surface of the obtainedTeO_2 after calcinations. Figure 6 shows the high-resolution XPS spectra of Cl, O, and Te measured on the surface of the calcined samples prepared with ethanol (sample Tol-1c) and water (sample Toh-2c), respectively. The weak Cl 2*p* signal indicates there is trace of Cl. TeO_2 prepared from $Te_6O_{11}Cl_2$ shows two stronger Cl 2*p* signals than the calcined TeO_2 prepared with water (Fig. 6), which implies there is trace Cl on the surface. The signal for Cl at 196.6 eV is ascribed to the ionic (Cl^-) [17]. According to the references, the Cl signal of Pb–Cl and Cu–Cl were reported at 198.3 [18] and 198.7 eV [19, 20], respectively. So the strong peak at 198.6 eV is ascribed to

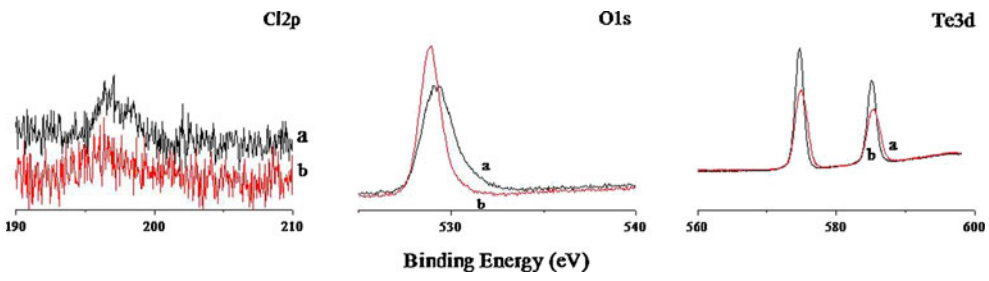

Fig. 6 The Cl, Te, and O XPS spectra of TeO_2Cl_x (sample Tol-1c) (**a**) and TeO_2 prepared with water after calcinations (**b**), respectively

the Cl of Te–Cl bond. Te 3*d*3/2 signals of TeO_2 prepared from $Te_6O_{11}Cl_2$ are at 529.2 and 574.9 eV, respectively. While the O 1*s* and Te 3*d*3/2 signals of TeO_2 (Sample Toh-2c) are at 528.8 and 574.7 eV, respectively. The signal at 574.9 and 574.7 eV are ascribed to Te–O bond [21]. It can be seen that there is no considerable shift of the peaks of Te 3*d* at all, which may be because there is trace Te–Cl bond. The shift of O 1*s* signals might be ascribed to the oxygen contamination. It was reported that the shift of O 1*s* signals was presumably associated with the oxygen and CO_2 adsorbed during the preparation of samples for XPS [22].

Various lithium-ion battery cathode materials have been improved by chlorine doping for different reasons. The reversible capacity and cycle stability of $LiNi_{0.7}Co_{0.3}O_2$ are improved for expanding the cell volume and decreasing the oxidation state of cobalt and nickel ions [23]. $Li_{1.06}Mn_2O_{4-z}Cl_z$ shows excellent cycle ability not only at ambient temperature but also at 55 °C for changing lattice parameter of spinel [24]. Also, the particle-to-particle impedance can be decreased by Cl^- substitution, resulting in greater reversibility for $LiV_3O_{7.90}Cl_{0.10}$ [25]. Cl^- doped $LiFePO_4$ also exhibits good electrochemical properties for the minor change of crystal structure and the increasing of Li^+ diffusion and exchange current density [26–28]. Here, the cyclic stability of TeO_2 anode material for lithium-ion battery is improved by chlorine doping, which promotes the formation of Li_xTe. The Te–Cl bond might play a great role in improving TeO_2 electrochemical properties.

Conclusions

In summary, $Te_6O_{11}Cl_2$ and TeO_2 microcrystals were prepared via a hydrothermal method with ethanol and water as solvent, respectively. After calcinations, both $Te_6O_{11}Cl_2$ and TeO_2 were converted to TeO_2Cl_x and TeO_2, respectively. The cell made from TeO_2Cl_x electrode material exhibits the highest discharge capacity and best cyclic stability than $Te_6O_{11}Cl_2$ and other TeO_2 due to Cl doping, which favors the formation of lithium–tellurium alloy and inhibits the formation of Li_xTeO_2.

Acknowledgments This work was supported by the funds (2010J05025, 2010-XY-5, and XRC-0926) and the open project in Key Lab Adv Energy Mat Chem (Nankai University) (KLAEMC-OP201201).

References

1. Champarnaud-Mesjard JC, Blanchandin S, Thomas P et al (2000) Crystal structure, raman spectrum and lattice dynamics of a new metastable form of tellurium dioxide: gamma-TeO_2. J Phys Chem Solids 61:1499–1507
2. Dewan N, Sreenivas K, Gupta V et al (2008) Comparative study on TeO_2 and TeO_3 thin film for gamma-ray sensor application. Sensor Actuat A-Phys 147:115–120
3. Dewan N, Sreenivas K, Gupta V (2008) Anomalous elastic properties of RF-sputtered amorphous TeO_{2+x} thin film for temperature-stable SAW device applications. IEEE T Ultrason Ferr 55:552–558
4. Singh AK, Rai SB, Rai DK, Singh VB (2006) Upconversion and thermometric applications of Er^{3+}-doped Li:TeO_2 glass. Appl Phys B-Lasers Opt 82:289–294
5. Murugan GS, Fargin E, Rodriguez V et al (2004) Temperature-assisted electrical poling of TeO_2-Bi_2O_3-ZnO glasses for non-linear optical applications. J Non-Cryst Solids 344:158–166
6. Murugan GS, Ohishi Y (2004) TeO_2-BaO-SrO-Nb_2O_5 glasses: a new glass system for waveguide device applications. J Non-Cryst Solids 341:86–92
7. Elsabawy KM, El-Hawary WF, Maghraby AE (2011) Cathodic capacity promotion via narrow range of nano-Te(IV)-dopings on $LiMn_{2-x}Te_xO_4$–spinel. Adv Appl Sci Res 2:1–8
8. Krins N, Rulmont A, Grandjean J et al (2006) Structural and electrical properties of tellurovanadate glasses containing Li_2O. Solid State Ionics 177:3147–3150
9. Wei HY, Lin J, Huang WH et al (2009) Mat Sci Eng B-Adv Func Solid-State Mater. 164:51–59
10. Di Giulio M, Zappettini A, Nasi L et al (2005) Rf-sputtering growth of stoichiometric amorphous TeO_2 thin films. Cryst Res Technol 40:1023–1027
11. Zhang HW, Swihart MT (2007) Synthesis of tellurium dioxide nanoparticles by spray pyrolysis. Chem Mater 19:1290–1301
12. Qin BY, Bai Y, Zhou YH et al (2009) Structure and characterization of TeO_2 nanoparticles prepared in acid medium. Mater Lett 63:1949–1951
13. Cho SC, Hong YC, Uhm HS (2006) TeO_2 nanoparticles synthesized by evaporation of tellurium in atmospheric microwave-plasma torch-flame. Chem Phys Lett 429:214–218
14. Ahmed MAK, Fjellvåg H, Kjekshus A (2000) Synthesis, structure and thermal stability of tellurium oxides and oxide sulfate formed from reactions in refluxing sulfuric acid. J Chem Soc Dalton Trans 2000:4542–4549
15. Feng ZB, Lin J, Wei HY et al (2009) Preparation of TeO_2 thin films from TeCl4 by non-hydrolytic sol–gel processing. J Chin Ceram Soc 37:1689–1693
16. Giester G (1994) $Te_6O_{11}Cl_2$—a revision of crystal symmetry. Acta Crystallogr C 50:3–4
17. AnY L, Tai NH, Chen SK et al (2011) Enhancing the electrical conductivity of carbon-nanotube-based transparent conductive films using functionalized few-walled carbon nanotubes decorated with palladium nanoparticles as fillers. ACS Nano 5:6500–6506
18. Hasik M, Bernasik A, Drelinkiewicz A et al (2002) XPS studies of nitrogen-containing conjugated polymers-palladium systems. Surf Sci 507:916–921
19. Sesselmann W, Chuang TJ (1986) The interaction of chlorine with copper 1. Adsorption desorption and surface-reaction. Surf Sci 176:32–66
20. Elzey S, Baltrusaitis J, Bian S et al (2011) Formation of paratacamite nanomaterials via the conversion of aged and oxidized copper nanoparticles in hydrochloric acidic media. J Mater Chem 21:3162–3169

21. Jeong SH, Lee JW, Ge DT et al (2011) Reversible nanoparticle gels with colour switching. J Mater Chem 21:11639–11643
22. Chen CW, Hsieh PY, Chiang HH et al (2003) Top-emitting organic light-emitting devices using surface-modified Ag anode. Appl Phys Lett 83:5127–5129
23. Li XL, Kang FY, Shen WC et al (2007) Improvement of structural stability and electrochemical activity of a cathode material $LiNi_{0.7}CO_{0.3}O_2$ by chlorine doping. Electrochim Acta 53:1761–1765
24. Liu WR, Wu SH, Sheu HS et al (2005) Preparation of spinel Li $(_{1.06})$Mn(2)O(4-z)Cl(z)cathode materials by the citrate gel method. J Power Sources 146:232–236
25. Liu L, Jiao LF, Sun JL et al (2009) Electrochemical performance of $LiV_3O_{8-x}Cl_x$ cathode materials synthesized by a low-temperature solid state method. Chin J Chem 27:1093–1098
26. Li N, Wu BR, Zhang CZ et al (2011) Research on the electrical electrochemical properties of the $LiFe_{0.98}Mn_{0.02}(PO_4)_{(1-0.02/3)}Cl_{0.02}$/C cathode materials. Adv Mater Res 287–290:1314–1321
27. Wang ZH, Yuan LX, Wu M et al (2011) Effects of Na^+ and Cl^- co-doping on electrochemical performance in $LiFePO_4$/C. Electrochim Acta 56:8477–8483
28. Sun CS, Zhang Y, Zhang XJ et al (2010) Structural and electrochemical properties of Cl-doped $LiFePO_4$/C. J Power Sources 195:3680–3683